"A Cochlear Nucleus Auditory prosthesis based on microstimulation"

Contract No. **No. NO1-DC-1-2105**

Final report

HUNTINGTON MEDICAL RESEARCH INSTITUTES

NEURAL ENGINEERING LABORATORY

734 Fairmount Avenue

Pasadena, California 91105

D.B. McCreery, Ph.D.

A.S. Lossinsky, Ph.D.

L.A. Bullara, B.S.

HOUSE EAR INSTITUTE

2100 WEST THIRD STREET

Los Angeles, California 90057

R.V. Shannon Ph.D

S. Otto M.S.

M. Waring, Ph.D

Jean Moore (consultant)

Table of contents

Review of workscope

The goal of Contract #NO1-DC-1-2105 has been to develop central auditory prostheses that utilize an array of microelectrodes implanted into the patient's ventral cochlear nucleus. The work scope has encompassed the following sub-tasks:

- Collaborate with the personnel at Cochlear Ltd. (Australia) and Cochlear Americas to complete the development of a human microstimulating array that contains 8 discrete activated iridium microelectrodes.

- Complete the development of a tool for inserting the electrodes into the human brainstem, and validate that the tool can be sterilized to the SAL 10^{-6} standard, using the equipment employed at the performance hospital.

- Collaborate with the clinicians at the house Ear Clinic, to evolve the method of implanting the penetrating array into the human auditory brainstem and develop methods of targeting the patient's cochlear nucleus after removal of vestibular tumors via the translabyrinthine approach

- Perform psychophysical evaluations of the first group of patients to receive the penetrating auditory brainstem implant array.

- Evaluate the electrical thresholds changes and tissue responses during the long-term (greater than 1 year) implantation of iridium microelectrodes into the feline cochlear nucleus.

- Begin the development of a 16-channel "second generation" microstimulating array for the cochlear nucleus that utilizes multisite silicon substrate probes developed at the University of Michigan. Here, the work scope is in the

preclinical phase and has used adult cats.

- Design and construct a module for our telemetrically-controlled backpack stimulator which allows 16 electrode sites to be pulsed independently.

I. Completing the development of the first penetrating microelectrode array for human use.

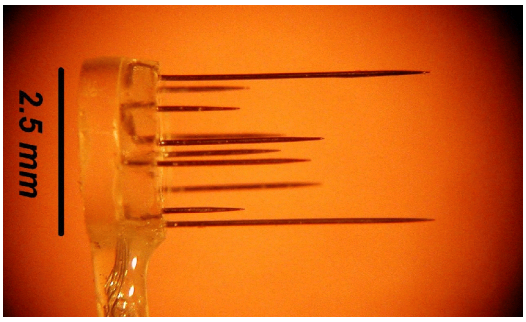

Fig 1

This is a continuation of work begun under the preceding contract. Fig. 1 shows the microelectrode array that is fabricated in Sydney, Australia by Cochlear Ltd. It contains 8 discrete activated iridium microelectrodes that range in length from 1-2 mm and also includes two longer (3-mm) electrically inactive anchoring pins which help to stabilize the array within the cochlear nucleus. The iridium microelectrodes are fabricated at HMRI. The physical configuration of the array is according to the specifications set forth by HMRI and HEI, and are based largely on the anatomical studies of Dr. Jean Moore, who remains a consultant to the project.

Early versions of the array were evaluated at HMRI and implanted into the cerebral cortex of a rabbit and into the spinal cord of a cat. Cochlear's quality assurance protocol requires that the implant must be fabricated using materials that are part of their quality control system. Thus, Cochlear and HMRI agreed that the array "button" (superstructure) should be fabricated from Epotek 301 epoxy, a U.S.P. Category VI material. Also, the electrode shaft are insulated with Parylene C. The adhesion of the Parylene to the iridium shafts is enhanced by pretreating the metal with a methyl silane (Silquest A174) which previously had undergone basic toxicity screening.

The personnel at Cochlear conducted accelerated electrical testing of the prototype devices. HMRI implanted two array using identical materials into the cerebral cortex of a New Zealand rabbit for 37 days (QPR #1) and a prototype array from Cochlear into the lumbosacral spinal cord in an adult cat, for 29 days (QPR #4). In the rabbit, there was minimal growth of connective tissue under the epoxy superstructure,

although the plane of the histologic section did not permit a precise measurement of the thickness of this capsule. The neuropil and neuronal density under the epoxy superstructure and around the penetrating electrodes was normal, and the tissue reaction around the electrodes treated with the Parylene adhesion enhancer (A174) was indistinguishable from the tissue response surrounding the untreated microelectrodes (QPR #1). In the cat spinal cord, the penetrating array was inserted using the handheld inserter tool that would be used to implant the array into the patient's cochlear nucleus. After 29 days, the connective tissue capsule under the array superstructure was approximately 200 μm in thickness with few inflammatory cells, indicating that this was the steady state condition. The neural tissue immediately beneath the capsule appeared healthy. There was some proliferation of small blood vessels around some of the electrode shafts. Overall, the histologic features of the implant sites were typical of those seen in the feline cochlear nucleus and spinal cord after implantation of microelectrode arrays fabricated entirely at HMRI.

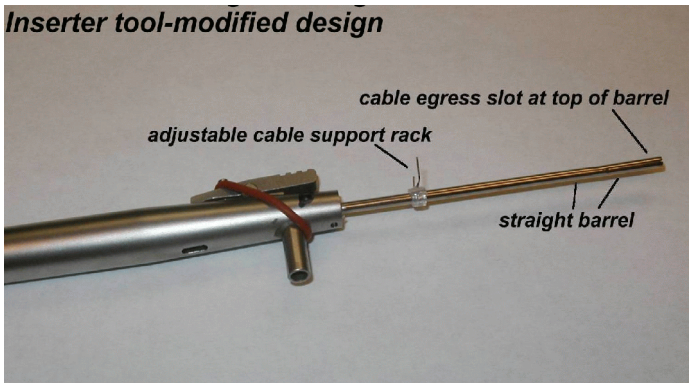

Fig 2

II. The array inserter tool: modifications and verification of sterilizeability.

The handheld array inserter tool is shown in Fig. 2. This tool contains a viscous damping mechanism that controls the velocity at which the array is inserted into the brain. Under this contract, we modified the damping mechanism in order to improve the sterilizeability and improve reproducibility of the insertion velocity. We commissioned a commercial testing laboratory (IBA Analytical Laboratories) to validate that the tool could be gas sterilized to the level required by the Food and Drug Administration ($SAL10^{-6}$; QPR #3).

III. Implantation of the penetrating array into human patients.

As of June 30, 2004, the 5 patients designated by the Food and Drug Administration under the feasibility IDE have received their implants. All of the patients were afflicted with type II Neurofibromatosis and the arrays were implanted following resections of a vestibular schwannoma via the translabyrinthine approach to the brainstem. The penetrating arrays were implanted by neurosurgeon William Hitzelberger at the St. Vincent's Medical Center. None of the patients have experienced any untoward effects that could be attributed to the implantation, residence or stimulation through the penetrating arrays. However, the problem of locating the small human cochlear nucleus has proved to be as difficult as originally anticipated, and remains a "work in progress". In all of these patients, the penetrating array and also an array of surface electrodes was implanted after removal of medium- to- large vestibular Schwannomas which can produce significant mechanical distortion of the adjacent brainstem. In the first 4 patients, the surgeon determined the point of insertion of the penetrating array based on landmarks on the surface of the brainstem. (Unlike the cat, the human cochlear nucleus is not a surface structure). In the 5th patient, the implantation was guided by electrically-evoked auditory brainstem responses induced using a handheld stimulator probe. The results from the first 5 patients are summarized below.

Patient #1 (QPR #9).

The first human implantation of an array of discrete iridium penetrating microelectrodes occurred on July 24, 2003. The procedure immediately revealed some problems with our strategy for targeting the ventral cochlear nucleus by using the Taenia choroidia as a landmark (the taenia is too wide in the rostral-caudal dimension) and with the routing of the cable from the penetrating array. Thus only one of the penetrating microelectrodes produced an auditory percept, and we did not achieve a true multi-channels device. However, the threshold of the auditory percept was low (< 1

nC), as predicted from the animal studies, and the dynamic range was quite large. The one electrode produce a high-pitched auditory percept. The patient has suffered no ill effects attributable to the penetrating array and is benefitting from the implant, which include both the penetrating electrodes and a surface electrode array. We then revised our procedure for targeting the human ventral cochlear nucleus and we have modified the inserter tool so that the cable from the penetrating array can pass over the surface of the brainstem.

Patient #2 (QPR #10).

After reviewing the intraoperative video from the first patient to receive the penetrating auditory brainstem implant array (PABI), we concluded that the placement of the penetrating array was a bit too caudal. We therefor elected to implant the array in PABI patient #2 in a slightly superior location, just dorsal to the root of the VIII nerve, and into the lateral wall of the nucleus, just dorsal of the taenia choroidia.

When PABI patient #2 returned for her hook-up 6 weeks after the surgery, she was getting good auditory sensations with low thresholds (1.7 nC/phase or below) from 5 of the 8 penetrating electrodes. One penetrating electrode induced dizziness at low stimulus amplitude, and the thresholds of the auditory percepts from two penetrating electrodes were close to the 3 nC/safety limits; they appear to be on the edge of the cochlear nucleus. She is perceiving a wide range of pitches (from 15 to 80 on a scale of 0 to 100) from the other 5 penetrating microelectrodes, and has a full range of loudness percepts, ranging from faint to loud, on all 5 channels, without exceeding the 3 nC/phase safety limit, and with no non-auditory percepts. With the penetrating electrodes, she achieved gap detection thresholds of 2 to 10 ms, which suggest very good temporal resolution.

The patient also had been implanted with an array of electrodes on the surface of the cochlear nucleus, and the auditory percepts were quite different for the surface and penetrating electrodes. In general, the penetrating electrodes produced sounds closer to pure tones (described as being like chimes or a calliope), which she found distracting, at least at first. However, by day 3, she apparently had begun to integrate

the percepts from the surface and penetrating electrodes, and by using a combination of 7 surface and 5 penetrating electrodes, she was able to achieve consonant and vowel recognition scores of 30- 35%, and modest open-set recognition of words in sentences

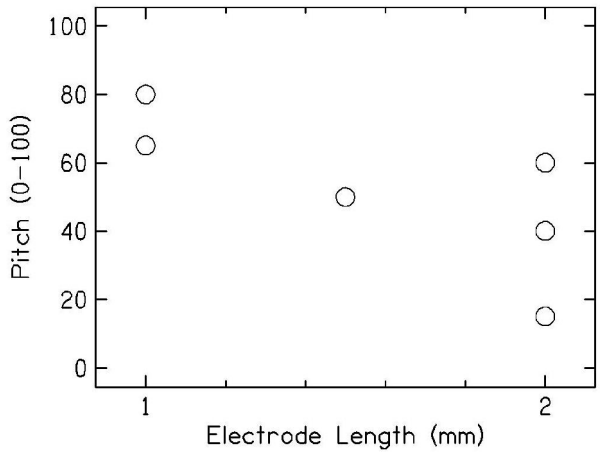

Fig 3A

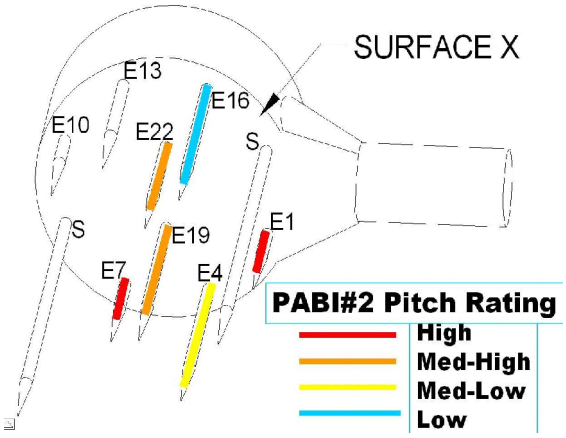

Fig 3B

(14%), which is exceptional performance for an ABI patient during initial testing. These results indicate that the targeting of the penetrating array into the cochlear nucleus was good at the time of surgery, that the array was inserted fully and stayed in place, and that the penetrating electrodes did not damage the neurons in the cochlear nucleus.

This patient has been very enthusiastic about the performance of the penetrating array and, in particular, she appreciates the range of pitch provided by various environmental sounds. She has stated that she even enjoys listening to music.

It is Instructive to note the distribution of pitch percepts from the penetrating microelectrodes of various lengths and positions on the array footprint (Fig. 3A & B). The array was implanted into the lateral surface of the cochlear nucleus and from the branching pattern of the human auditory nerve fibers, it is expected that this angle of insertion would cause the microelectrodes to cross the tonotopic strata at a highly oblique angle. Indeed, the data from patient #2 shows that the pitch percepts elicited by different microelectrodes is influenced both by the lengths of the microelectrodes

(longer electrodes tend to elicit lower pitch percepts) and by the electrode's point of entry into the nucleus.

Patient #3 (QPR #11).

Patient #3 received auditory percepts from 4 of the 8 penetrating microelectrodes. However, unlike patient #2, the penetrating microelectrodes did not improve his ability to recognize speech-related material. In this patient, the penetrating microelectrodes did not elicit the full range of pitch percepts seen in patient #2 (most elicited very low-pitched tones), and in particular, they did not elicit pitch percepts in the range of auditory frequencies that is critical for speech perception (although they may be helpful for perceiving and identifying environmental sounds). All of the functional penetrating microelectrodes were located on the anterior portion of the penetrating array. This patient illustrates the need for a more reliable means of targeting the penetrating array into the cochlear nucleus. At this time, Dr. McCreery began working with Dr. Waring at the HEI to develop a handheld stimulating probe for this purpose.

Patient #4.

This patient did not receive any auditory percepts from her penetrating microelectrodes. Dr. Brackmann has ordered plane film skull x-rays to determine if the penetrating array became dislodged during the terminal phases of the implant surgery. However, a review of the intraoperative video shows that the array was implanted slightly lateral of the tenia choroidea. This location is somewhat lateral of the implant site in patient #2.

Patient #5.

This patient is afflicted with a particularly severe form of NF-2 and at the time of surgery had tumors on most of his cranial nerves. The brainstem was significantly distorted after resection and/or debulking of the tumors. The new handheld stimulating probe was used to locate the site for implantation of the penetrating microstimulating array. The site from which the maximum EADR was elicited was somewhat medial of

the tenia choroidea and medial of the implant sites in the previous patients. The array was implanted at this site, in spite of some misgivings by the neurosurgeon that the site was too far medial. Subsequently, this patient did not receive auditory sensation from any of the penetrating electrodes. However, he did experience a pronounced tickling sensation in the throat from at least two of the penetrating electrodes. This indicates that the penetrating electrodes had remained fixed in the brainstem and that there were intact neurons subjacent to the array, but that the array had completely missed the cochlear nucleus, and in fact probably was close to the hypoglossal nucleus. This patient is a warning not to be led astray by the intraoperative evoked potentials, which can arise from brainstem nuclei other than the cochlear nucleus. The intraoperative EABRs still may be very useful in placing the PABI, but only if they are evoked from a site that is anatomically plausible.

Evoked Response Measures

Intraoperative electrically-evoked auditory brainstem responses (EABRs) were recorded from scalp electrodes during stimulation with both surface and penetrating electrodes in PABI patients #2 and #3. In PABI patient #2, post-operative EABRs were also recorded while stimulation with both penetrating and surface electrodes. No EABRs were observed while stimulating with the penetrating electrode in PABI#2, either intraoperatively or postoperatively. Clear stimulation artifacts were observed during the postoperative testing, indicating that stimulation was being delivered to the electrodes properly. However, even though auditory perception was achieved for seven of the eight penetrating microelectrodes, no EABRs were obtained that were reliable. A postoperative EABR from at least one surface electrode was observed and had a waveform morphology that was similar to that recorded during stimulation with the same electrode during surgical placement. In PABI patient #3, EABRs evoked from most of the surface electrodes were recorded intraoperatively but no reliable EABRs were observed while stimulating with most of the penetrating electrodes. A small EABR from one penetrating electrode was detected intraoperatively, but we will not know until initial stimulation (Mid-March 2004) if that electrode produces auditory sensations. In general,

it appears that intraoperative monitoring of EABRs is effective for assistance in positioning the surface ABI array, but may not be as useful for assisting the placement of the penetrating array. A large evoked potential recorded from patient #5 and evoked by a hand-held probe proved to be a miscue, and the array apparently was implanted close to the hypoglossal nucleus rather than into the cochlear nucleus. We will continue to measure intraoperative and post-operative EABRs from penetrating electrodes in an attempt to improve recording parameters and techniques.

Post-Operative Imaging

In PABI patient #1 we attempted to document the location of the PABI electrodes using interleaved CT imaging sequences with double contrast. Although CT images do not show soft tissue structures, we have shown in the past that it is possible to determine if surface ABI electrodes are in the vicinity of the lateral recess of the IV ventricle by assessing their location relative to bony landmarks. Repeated imaging sequences over time can show movement of electrode assemblies relative to bony landmarks. Unfortunately, we were unable to visualize the penetrating electrodes of the PABI in CT images in PABI#1.

In PABI patient #2 we tried to document/quantify the location and orientation of the penetrating electrode assembly using standard views with high resolution plain film X-rays. The images did have sufficient resolution to see the individual microelectrodes in the penetrating array and the relative position and orientation of the array could be documented. We hope to repeat such images in subsequent PABI patients to see if they can provide verification of good vs poor electrode placement and to verify electrode stability over time.

Summary (Sections I - III)

We have completed the development of the first generation microstimulating array for the human cochlear nucleus, and the tool for implanting the array, and we have implanted the device into 5 patients. Not of the patient have experienced any untoward effects that can be attributed to the penetrating electrodes. The data from patient #1,2,and 3 indicates that the penetrating electrodes do induce auditory percepts with charge thresholds very close to what was predicted from the response growth functions induced by microelectrodes implanted chronically in the ventral cochlear

nucleus of cats. The patients perceived pure tones, and for patient #2, the pitch differed for different microelectrodes, also as predicted from animal studies, and the anatomy of the human auditory system. The penetrating array has accorded her modest improvement in speech perception over what has been seen previously in patients implanted only with the surface array, and in her e-mails she has expressed her appreciation for the range of pitch percepts from the penetrating array, when she listens to environmental sounds.

In at least 4 of the 5 patients, the testing at 90+ days after implantation showed that the microelectrodes remained in the brainstem, in spite of the challenging issues related to cable routing. This justifies the basic design of the penetrating array, including the use of the long stabilizing pins.

The problem of locating the small ventral cochlear nucleus has emerged as a significant problem, which remains unresolved at this time. It is hoped that by using a combination of anatomical landmarks and interoperative evoked potentials, we can devise a reliable strategy for locating the point of implanting the array, even in these patients in which the surface of th brainstem has been significantly distorted by the large tumors.

IV. Evaluation of long-term implantation of microelectrodes into the feline cochlear nucleus.

As part of our evaluation of the safety of prolonged implantation and stimulation of intranuclear microelectrodes, we utilized 2 cats (CN-139 and CN-140) that had discrete iridium microelectrodes implanted into their cochlear nucleus during the preceding contract cycle.

We sacrificed cat cn139 at 53 months after implanting 3 iridium stimulating microelectrodes into its posteroventral cochlear nucleus. The electrodes were insulated with Epoxylite 6001 electrode varnish. The threshold of the electrical response evoked from the microelectrodes had remained quite stable throughout the period of implantation, but over the course of the 53 months, the connections to two of the 3 electrodes failed at the junction with the percutaneous tower, and this was the basis of

the decision to sacrifice the cat. During the 2.5 years *in vivo*, the threshold of the evoked response increased slightly, from about 6 μA to approximately 8 μA. This longevity of the intranuclear electrodes is similar to that seen in previous long-term implants in our cats. Histologic evaluation of the electrode sites revealed that the upper parts of the Epoxylite-insulated electrode shafts were surrounded by a chronic inflammatory process, similar to what we have observed previously. Its frequent occurrence appears to justify our decision to insulate our electrode shafts with Parylene-C rather than with Epoxylite. Deeper in the nucleus, the sheath around the electrodes was thinner and there was less evidence of the chronic inflammation. The tip sites of all of the microelectrodes were surrounded by a very thin gliotic sheath. Outside of this capsule, the neuropil and neurons ventral to the tip site was somewhat compressed and distorted ventrally but otherwise appears to be normal and healthy. These findings are consistent with the good stability of the evoked responses over the period of implantation.

The stability of the compound action responses evoked in the cochlear nucleus and recorded in the contralateral inferior colliculus is notable, since this cat had undergone 3 regimens of prolonged stimulation, including a 21-day regimen using stimulus parameters exceeding those now being used in human patients (QPR #3).

We also sacrificed cat CN140 at 1125 days after implanting 3 microelectrodes into the posteroventral cochlear nucleus (PVCN). This cat had not been subjected to regimens of prolonged stimulation. The potentials evoked from the microelectrodes in the PVCN and recorded in the contralateral inferior colliculus were comparable at 17 days and at 1125 days after implantation of the array. The histologic evaluation of the microelectrode tracks and tip sites showed a thin (less than 25 μm) gliotic capsule surrounding the microelectrodes with normal-appearing neurons and neuropil immediately adjacent to the capsule. Overall, the small changes in the evoked response during the period of implantation and the histologic findings of the electrode sites were similar to those from cat CN139, which had undergone several sessions of prolonged stimulation during a comparable period *in vivo*.

V: Evaluation of chronically-implanted silicon-substrate microelectrode arrays

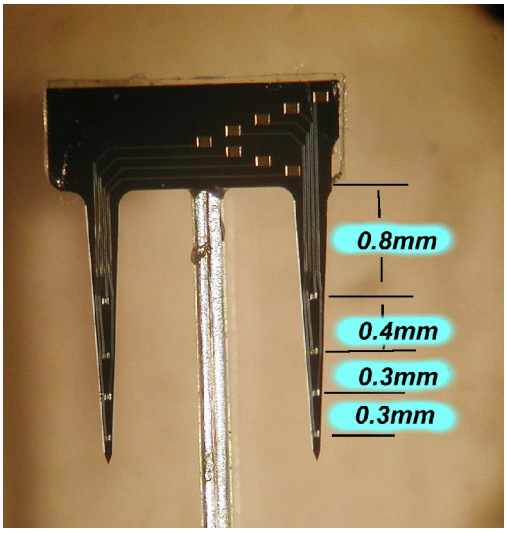

Fig 4A

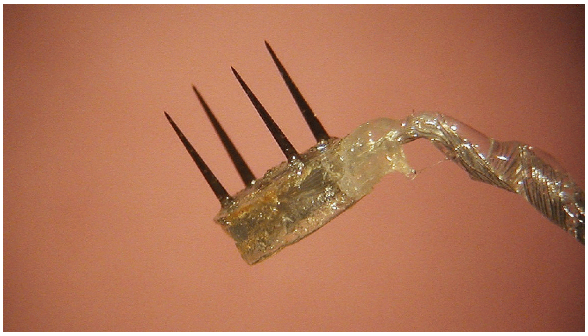
Fig 4B

The workscope of this contract calls for the development of arrays of silicon substrate electrodes, which should allow placement of many more electrode sites into the human cochlear nucleus than is possible with discrete iridium microelectrodes. We are developing an array for implantation into the human cochlear nucleus that has 16 electrode sites distributed on 4 silicon shanks extending from an epoxy superstructure that is 2.4 mm in diameter. This is the same footprint as our first-generation human arrays employing discrete iridium microelectrodes and is designed to be implanted using the same inserter tool. The silicon probes are fabricated at the University of Michigan under the direction of Design Engineer Jamille Hetke. Figure 4A shows a probe with 2 shanks and 8 stimulating sites, that have been sputter-coated with iridium oxide. The 4 sites on each shank are located between 0.8 to 1.7 mm below the top of the shanks. Figure 4B shows an array with 2 of the probes (4 shanks and 16 electrode sites) extending from an epoxy superstructure that floats of the surface of the cochlear

nucleus. The cable is angled vertically, to accommodate the trans-cerebellar approach to the feline cochlear nucleus.

Using aseptic technique, the cat's scalp is opened in a midline incision, and the muscles reflected. A small craniectomy iss made over the right occipital cortex and the bipolar recording electrode iss introduced into the rostral pole of the right inferior colliculus.To access the cochlear nucleus, a craniectomy iss made over the left cerebellum, extending up to the tentorium. The rostrolateral portion of the left cerebellum is aspirated using glass pipettes. The electrode array is secured on the end of a vacuum wand, and thereby advanced into the cochlear nucleus.

In cats CN142, 143 and 144, we inserted the arrays into the cochlear nucleus in a near dorsal-ventral orientation, so that the electrodes would cross the isofrequency lamina at a steep angle. Cat CN142 was maintained for 63 days after implanting an array of 4 silicon substrate shanks and 16 simulating electrodes sites into the posteroventral cochlear nucleus. At autopsy, it was determined that the two rostral silicon shanks were within the PVCN. The histologic evaluation of the implant site suggests some loss of neurons within 50 μm of the silicon shanks, but the thresholds of the potentials evoked from all of the microelectrode sites in the PVCN stabilized after approximately 42 days in vivo, at values comparable to what we had previously measured for discrete iridium microelectrodes implanted chronically in the feline PVCN.

At 63 day after array implantation, the ability of the ensemble of microelectrode sites to access the tonotopic organization of the PVCN was evaluated by recording the compound action potentials evoked from each of the microelectrode sites, at a sequence of depths along the dorsolateral-ventromedial axis of the contralateral. We showed that the ensemble of microelectrode sites was able to excite separate populations of neurons in the PVCN, and was able to access the tonotopic organization of the PVCN in an orderly manner. This was determined by current density analysis of the serial depth recordings made in the contralateral inferior colliculus.

In cat CN145, we inserted the array into the cochlear nucleus at angle of approximately 45 degrees from the vertical. This was done so that the array could be inserted into the lateral wall of the cochlear nucleus and the underside of the array

superstructure would be nearly parallel to the dorsolateral surface of the nucleus, which slopes at a steep angle. As noted above, our experience from the first two human patients suggest that it will be preferable to insert the arrays into the lateral surface of their ventral cochlear nuclei.

About 24 hours after implanting the array, the neuronal activity induced by 8 of the silicon sites was mapped in the contralateral inferior colliculus by recording the compound action potentials evoked by a stimulus current of 20 μA in the ventral cochlear nucleus (biphasic, controlled-current pulses of 150 μs/phase). Recordings were made at intervals of 100 μm along the dorsolateral to ventromedial axis of the IC, between the surface and a depth of 4,800 μm. The source of neuronal activity was localized using current source density analysis. The results of this analysis were consistent with the cochleotopic organization of the feline cochlear nucleus as demonstrated previously by other workers, using anterograde tracers injected into the cochlea. We showed that access to the tonotopic axis of the cochlear nucleus still is possible with the low-angle approach, particularly in the caudal part of the nucleus (the posteroventral cochlear nucleus). However, with this orientation of the silicon shanks, there is significant overlap of the frequency bands excited by adjacent electrode sites on a particular shank. Also, more than one shank will be required to access the entire tonotopic axis. This was confirmed in cat CN147. The results from that animal are presented in greater detail in Section VI of this report.

High-speed insertion of the silicon-substrate array- effects on surface vasculature and response of the shanks to mechanical stress

Implantation of any microstimulating array into the human cochlear nucleus through the narrow opening of the translabyrinthine approach can be accomplished only with the aid of a hand-held inserter tool. The requirement that the tool must be supported in the surgeon's hand dictates that electrode insertion occur at a moderately high speed (full insertion within a few ms). However, insertion at high speed may subject the silicon array shanks to greater mechanical stress than would insertion at slower speed. We have selected the feline lumbosacral cord as a model for the human

auditory brainstem because of its many anatomical similarities, including a thickened glial membrane and some large blood vessels on its dorsal surface. The 3 mm silicon probes (sized for the human cochlear nucleus) are somewhat longer than those that we have previously implanted into the feline cord so we evaluated 2 of these arrays for mechanical integrity.

A cat was anesthetized with Halothane and the lumbosacral cord was exposed by a standard dorsal laminectomy. The 2 arrays of 2 probes (4 shanks) were inserted into the cord's dorsal surface a total of 18 times using the handheld electrode inserter tool developed for the human cochlear nucleus. We attempted to impale the large midline artery on the cord's dorsal surface, and we achieved this a total of 6 times with the 2 arrays. The impaled artery did not bleed while the array was *in situ* but it did bleed profusely after the array was removed. However, in all cases, bleeding ceased within 10 seconds after removal of the array, and blood continued to flow through the artery. .

Array #1 was implanted and removed 9 times. On the 6th implantation and removal, one of the shanks fractured from the array, at the level of the epoxy superstructure. On the 9th insertion and removal, a second shank fractured midway between the tip and the superstructure. One shank fractured from array #2 during the 6th insertion and removal. It is not certain if the shanks fractured during implantation or during the subsequent removal. Thus the shanks of the 3 mm probes did withstand insertion and removal from the spinal cord, but they did eventually fail, probably as a result of accumulated stress and microfractures.

Reinforcing and tethering the silicon shanks

As noted above, there is a chance that the silicon shanks will fracture and detatch from the array during implantation. We have been investigating procedures for tethering the shanks of the silicon substrate probes so that if they do fracture from the superstructure, the detached shanks or fragment does not migrate down into the brain. We have determined that an epoxy backing will delaminate from the shanks after 30 days *in vivo*, so this type of backing is not a reliable method of restraint. We

encapsulated the probe shanks within 3-4 μm of Parylene-C, and then ablated the Parylene from the electrode sites with an excimer laser. This worked well, without damaging the probe or the photolithographic features. The probes were then intentionally fractured. When the probes were stressed at a right angle to the plane of the probe, the Parylene remained as an intact hinge which tethered the probe. However, when the probe was deflected to either side, the hinge of Parylene was torn. This demonstrated that 4 μm of Parylene-C will not yield a reliable tether (QPR #4).

We have evaluated the tensile properties of a film of flexible (20 durometer) silicone-elastomer applied to the unfeatured side of the probes. Silicone elastomers are capable of bonding covalently to the rigid silicon substrate, so the attachment between this film and the substrate coating should be very stable during prolonged soaking *in vivo*. When the silicon probes were intentionally fractured, the adherent film of silicone elastomer formed a durable hinge, with sufficient tensile strength to prevent a fractured probe from detaching completely from the array superstructure (QPR #5). However, this does not solve the underlying problem of the probe fracturing.

VI: Results not previously reported

An electrode array with 2 of the 2-mm probes was implanted into the cochlear nucleus of a young female cat (CN147). In two previous animals, the array was implanted at a high angle (close to the vertical) so that the silicon shanks would traverse the isofrequency lamina of the ventral cochlear nucleus at a steep angle. In previous animals, we had inserted the arrays into the cochlear nucleus in a near dorsal-ventral orientation, so that the electrodes would cross the isofrequency lamina at a steep angle. In CN147, the array was implanted into the dorsolateral surface of the nucleus at an angle of 45° from the vertical, to allow the underside of the array to lie nearly flat on the sloped dorsolateral surface of the nucleus, rather than having the lateral surface of the array elevated off of the nucleus.

Using aseptic technique, the scalp was opened in a midline incision, and the muscles reflected. A small craniectomy was made over the right occipital cortex and the bipolar recording electrode was introduced into the rostral pole of the right inferior

colliculus. The reference electrode was dorsal to the colliculus. These electrodes are solid 100 µm ss wire, with ~ 1 mm of the Teflon insulation removed for the tips.

To access the cochlear nucleus, a craniectomy was made over the left cerebellum, extending up to the tentorium.

The rostrolateral portion of the left cerebellum was aspirated using glass pipettes. The electrode array was secured on the end of a vacuum wand, and thereby advanced into the cochlear nucleus. Before releasing the vacuum, the array cable was fixed to the bone at the margin of the craniectomy, using medical grade SuperGlue and the cavity was filled with gelfoam.

Periodically, the responses evoked from each of the microelectrodes in the left cochlear nucleus were recorded via the electrode in the rostral pole of the right inferior colliculus. The stimulus was cathodic-first, charge-balanced pulse pairs, each phase 150 µs in duration, ranging from 0 to 35 µA in amplitude. 512 to 2048 successive responses were averaged to obtain each averaged evoked response (AER). The response growth functions, which represent the recruitment of the neural elements surrounding the microelectrode, were generated for each stimulating electrode site in the PVCN, by plotting the amplitude of the first component of each of the AERs evoked from that site, against the amplitude of the “probe” stimulus that evoked the AER.

Forty-seven days after implanting the array, the cat was sacrificed for histologic evaluation of the implant site. This sacrifice time is appropriate to observe the sub-acute phase of the tissue response to the implant, the extent of connective tissue growth under the array button and evidence of damage to blood vessel during the insertion process (hemosiderin from extravasate blood will remain in the tissue at this time). The cat was anesthetized with pentobarbital, given 5,00 units of heparin, and perfused with 250 ml of saline prewash through the ascending aorta, then with 3 - 4 L of fixative (4% paraformaldehyde in 0.1 M sodium cacodylate buffer, pH 7.4) using a peristaltic pump at 120 mm Hg. Following perfusion the head with the electrode array *in situ* was left in fixative until autopsy the following day.

Tissue containing the tracks of the silicon shanks was resected as a single block and embedded into paraffin, then sectioned at a thickness of 8 µm and stained with

cresyl violet (Nissl stain) for assessment of neural elements. The sectioning was done in the frontal plane, approximately parallel to the tracks of silicon shanks.

Prior to sacrificing the animal, we mapped the responses in the inferior colliculus while stimulating in the cochlear nucleus via the various electrode sites on the array implanted in the CN. It is well established that high and low acoustic frequencies from the basal and apical cochlea map onto a dorso-to-ventral tonotopic gradient in the ventral cochlear nucleus and that this ordered representation of acoustic frequencies then projects (in an inverted manner) onto the central nucleus of the inferior colliculus, with low acoustic frequencies represented in the dorsolateral part of the IC's central nucleus and high frequencies in the ventromedial portion (e.g, Semple and Aitkin, 1979).

The inferior colliculus mapping was done with the cat anesthetized with isoflurane and oxygen. The stimulus current was 20 μA, with a 150 μs/phase duration, at 50 Hz. The response from 11 electrodes sites in the ventral cochlear nucleus were mapped at 200 μm increments of depth along the dorsolateral-ventromedial axis of the IC, from the surface to a depth of 4.8 mm. The responses from all sites was acquired before the depth of the recording electrodes was advanced. The response to 512 successive stimuli were averaged, at each depth in the IC and for each electrode site in the CN.

Current source density (CSD) analysis proven useful for localizing coherent induced neural activity. The technique locates regions within the tissue volume in which current is passing from the extracellular compartment into (or out of) a spatially extensive intracellular compartment. The CSD at point x,y,z within the tissue volume represents the net current flowing in or out of the neural elements and is given by:

$$I_{d(x,y,z)} = -[\, \sigma_x \, \delta^2 \phi/\delta x^2 + \sigma_y \, \delta^2 \phi/\delta y^2 + \sigma_z \, \delta^2 \phi/\delta z^2 \,] \quad (1)$$

where ϕ is the field potential at x,y,z, and σ_x, σ_y and σ_z are the principal tissue conductances (Freeman and Nicholson, 1975). To compute equation 1, the extracellular field potential must be measured simultaneously at 7 (or more) points, at

and around x,y,z. However, in situations in which the neuronal responses to the stimulation are quite constant over time and in which the tissue is nearly isotropic ($\sigma x \cong \sigma y \cong \sigma z \cong \sigma$) as in the central nucleus of the inferior colliculus (Harris, 1987), then the current source density can be computed from measurements of the averaged evoked potential obtained along a single axis. The representation of sound frequencies determined with this approach are consistent with the known organization of the central nucleus of the inferior colliculus (Harris, 1987) and very similar to the results obtained using simultaneous multi-unit analysis (McCreery et al, 1998).

Freeman and Nicholson (1975) compared various smoothing procedures for reducing the noise inherent in the calculation of the 2nd spatial derivative of ϕ, while maintaining the essential spatial resolution. The 5-point finite approximation appeared to be the most useful:

$$I_{d(x,y,z),} \cong D(x,y,z) = (0.01\ \sigma/h^2)[-2\phi(x-2h) - \phi(x-h) - 2\phi(x) + \phi(x+h) + 2\phi(x+2h)] \quad (2)$$

Here, h is the spacing between the points at which the instantaneous field potential ϕ is measured. This formula is computationally equivalent to obtaining a least-squares error fit of a cubic polynomial to 5 successive data points along the axis of measurement, and then computing the second derivative of the fitted polynomial. We have used this version of CSD to demonstrate that intranuclear microstimulation with discrete iridium microelectrodes can access the tonotopic gradient (McCreery el al, 1998). We did not measure the conductivity of the living tissue in the inferior colliculus, and therefore, the CSD is expressed as arbitrary units, with a maxima of 2000 and minima of - 2000.

RESULTS

Fig. 5A shows a histologic section through the left cochlear nucleus. The upper portion of the tracks of the caudal-lateral (CL) and caudal-medial (CM) silicon shanks are visible as they enter the posteroventral cochlear nucleus. The dorsolateral surface of the nucleus has been flattened markedly and depressed by the underside of the

array's superstructure. We have seen this phenomenon previously and it undoubtedly can be attributed to continued downward force exerted by the rather thick and stiff array cable. Unlike the human array, in which the cable traverses laterally in the plane of the superstructure, the cable of the cat implant is directed upwards (Fig. 4B above) in order to accommodate the transcerebellar approach into the cochlear nucleus. Also, the cable is anchored to the bone at the point in which it exits the craniectomy. Thus, the array cannot truly float on the surface of the nucleus, and the problem probably is exacerbated by the presence of 16 conductors in the cable, which adds to its stiffness, And for the tendency of silicon elastomers to absorb water and expand slightly after implantation. In future arrays, we will attempt to improve the cable's compressibility by omitting the silicon rubber coating on the terminal 10 mm and by increasing the diameter of the cable.

Fig. 5B is a section slightly rostral to 5A, showing the site of the tip of the caudal-lateral shank and a deep segment of the rostral-medial shank. The tips of both shanks have passed completely through the cochlear nucleus.

Fig. 5C shows a section of the track of the caudal-lateral shank, at higher magnification. There is a marked inflammatory response around this and portions of the other shanks. This may in part be a response to the ongoing localized tissue injury as the array button sinks into the tissue, but it is seen along the full length of the shafts and is not confined to the regions of the tips where one would expect the greatest injury associated with continuous movement. Fig. 5D shows a cluster of new hyperplasic blood vessels near the point of entry of the caudal-medial shank. The vessels are surrounded by numerous macrophages ("perivascular cuffing"), a phenomenon that is indicative of an ongoing inflammatory response. In this implant, the silicon shanks were coated with albumen in the hope of preventing deposition of decomposed Epotek 301 epoxy that was generated during some laser machining operations conducted late in the fabrication process. It is possible that some residue from this material escaped the final cleaning process, which must be very gentle in order to avoid fracturing the silicon shanks. We have redesigned the array fabrication process, and we have eliminated the need for the laser machining step after the Epotek button has been cast.

Fig. 5E shows the connective tissue capsule under the array superstructure, in a region in which it did not delaminate from the brain during removal of the array. The capsule is less than 100 μm in thickness, and this probably represents a steady state condition at 47 days after implantation. The subjacent neurons and neuropil (in this case, in the dorsal cochlear nucleus) appear healthy and normal.

Fig. 5F shows the track of the rostral-lateral and rostral-medial shanks. The rostral-medial shank has passed through the dorsal cochlear nucleus and into the anteroventral nucleus, and the rostral-lateral shank has passed through the root of the auditory nerve. Fig. 5G is a section very near the tip of the 2 rostral shanks. Like the caudal shanks, their tips have passed completely through the cochlear nucleus as the surface of the nucleus was compressed by the underside of the array superstructure.

Fig. 5-11 shows, at higher magnification, the tissue surrounding the rostral-medial shank in the AVCN. Despite the ongoing inflammatory response, the neuropil within 50 μm of the track appears healthy and there are normal-appearing neurons within 100 μm of the track.

Overall, in spite of the problems related to the inflammatory response around the silicon shafts and the compression of the surface of the nucleus by the array superstructure, the cochlear nucleus is intact and the neurons and neuropil appear to be quite healthy and normal. None of the histologic sections revealed microhemorrhages, space-occupying glial scars or other indications of extravasated blood cells (e.g., hemosiderin).

Fig. 6 shows the location of the 16 stimulating electrode sites on the 4 silicon shanks. Fig. 7 shows the response growth functions of the first component of the evoked response recorded via the electrode chronically implanted in the rostral pole of the right inferior colliculus, while stimulating with the silicon electrode in the left cochlear nucleus. The responses from the caudal-lateral shank (Fig. 5A-B), the caudal-medial shank (Fig. 7C-D), the rostral-lateral shank (Fig. 7E-F) and the rostral-medial shank (Fig. 7G-H) are shown. The upper and lower panels show data acquired one day and 47 days after the implant surgery, respectively. The subsidence of the array into the cochlear nucleus is reflected in the changes in the RGFs between days 1 and 47. For

example, the threshold of the RGF from the deepest site on the rostrolateral shank (site 16) increased from about 10 μA on day 1 to more than 35 μA on day 47 (Fig. 7A-B) as the shank penetrated completely through the PVCN (Fig. 5B). A similar phenomenon occurred with electrode site 9 (the second deepest on the caudal-medial shank, as shown in Fig. 7C & D). Apparently, site 13 was deep to the PVCN, even immediately after implantation. Note that the histologic section in Fig. 5B does not show the deepest point of the caudal-medial shank.

The separation between the RGFs evoked from the different sites in the cochlear nucleus is an indication of the capacity of the different sites to excite different populations of neurons (note that the sites are spaced 300-400 μm apart along the shanks, beginning 800 μm below the underside of the array superstructure; Fig. 4). It is notable that the threshold of most of the RGFs was close to 5 μA in spite of the ongoing inflammatory response around the silicon shanks.

Fig. 8A and 8B show families of evoked responses recorded along the dorsolateral-ventromedial axis of the right inferior colliculus during the terminal experiment, 47 days after the implant surgery. The stimulus amplitude was 20 μA. The responses were measured at interval of 200 μm along the track through the IC. Responses from a site on the caudal-medial shank in the PVCN and from a site at approximately the same depth on the rostral-medial shank (in the AVCN) are shown.

Current sinks (negative values of CSD) occur when membrane depolarization causes ionic currents to flow into a neuron. Current sinks are commonly equated with regions of excitatory synaptic activity. Under these conditions, the spatially adjacent current sources represent the return of this current to the extracellular compartment, through passive membrane. Sinks also may be generated by synchronous action potentials, wherein the spatially adjacent current sources represent the return of the current to the extracellular compartment through passive neuronal membrane, and the temporally adjacent sources represent repolarization of the active neuronal membranes. However, current sources also may be generated by inhibitory post-synaptic activity (ipsp's), with the associated sinks representing passive inflow of this current. The current sinks and sources were computed from the families of evoked potential, using

equation 2. Fig. 9 shows contour maps (in arbitrary units) of the current sources and sinks evoked from all 11 of the electrode sites in the cochlear nucleus for which the evoked response threshold was 20 μA or less. The largest current sink is associated with the prominent negativity in the evoked responses, at about 3.5-3.88 ms after the stimulus pulse pair in the cochlear nucleus (Fig. 8). Fig. 10 shows the distribution of the depths of the current sinks in the IC for all 11 of these electrode sites. The bands span the amplitudes of the major sink near 3.5 ms, and the portion of the amplitude range between -1000 and -2000. Collectively, these sinks from the 11 sites span most of the depths of the central nucleus of the IC and correspond to acoustic frequencies up to approximately 10 KHz (Brown et al., 1997). The current syncs for many of the sites on the same shank are at similar depths in the IC and this indicates that they are exciting neurons in similar isofrequency lamina in the PVCN or AVCN. The shafts penetrated into the cochlear nucleus at an angle of approximately 45 ° from the vertical, which is more- or- less parallel to the isofrequency lamina (Leake and Snyder, 1989; Snyder et al, 1997). It is notable that in human patient #2, there was a tendency for the longer microelectrodes to induce lower pitch percepts but also a strong dependence upon the point of penetration of the electrode into the cochlear nucleus, a situation analogous to the scheme depicted in Fig. 10. It is worthwhile to speculate on the value of an auditory prosthesis that can independently excite not only different isofrequency lamina in the CN but also different portions of a particular isofrequency lamina. For example, Leake & Snyder (1989) showed that spiral ganglia neurons that lie close to the scala vestibuli project to the medial portion of each isofrequency lamina in the cochlear nucleus while the spiral ganglia cells closer to the scala tympani project to the lateral portion of each lamina, at least in the high frequency portion of the cat's cochlea. It is quite probable that different portions of each isofrequency lamina subserve different functions.

Summary (Sections IV- VI)

We have been developing a 16-site microelectrode array for the cochlear nucleus that is based on a pair of 8-site, 2-shank silicon probes fabricated and provided by the

CNCT at the University of Michigan. We have demonstrated that the array can be implanted into the feline spinal cord using the same handheld inserter tool that is used to implant the first generation device described in Sections 1, 2 and 3 of this report. Problems related to the fragility of the silicon shanks have been identified and will be addressed in the next contract cycle. We also are developing a version of the array that is suitable for implantation into the feline cochlear nucleus, and 6 of these have been implanted into young adult cats, for up to 1 year. Two cats remain alive and healthy at the time of this writing. The threshold of the compound action potentials from the implanted arrays has been comparable to what we have seen previously with chronically implanted discrete iridium microelectrodes.

We have noted a tendency for the chronically-implanted electrode arrays to depress the dorsolateral surface of the cochlear nucleus. We have found that this will occur when there is a small but continuous downward pressure of the array against the surface of the brain. In this case, the offender appears to be the array cable which is routed upwards and is anchored in the bone during the implant surgery, in order to accommodate the transcerebellar approach into the feline cochlear nucleus. The problem may be exacerbated by the tendency for the silicone elastomer which coats the cable to absorb water, causing the elastomer to expand and the cable to lengthen slightly. The cable has been modified in an effort to eliminate this problem.

We have demonstrated that individual electrode sites on the silicon shanks can excite different populations of neurons in the cochlear nucleus, even at an amplitude of 35 μA (5.2 nC/ph), which is in excess of the maximum charge that is now being used in the human patients.

In the most recent 3 cats, the arrays have been implanted so that the shanks are nearly perpendicular to the dorsolateral surface of the cochlear nucleus, which allows the underside of the array button to rest flat on the surface of the nucleus, but which has made it difficult to access separate isofrequency lamina via the different sites on each silicon shank. Based on the branching pattern of the human auditory nerve in the cochlear nucleus, the isofrequency lamina in the human and feline ventral cochlear nuclei are roughly similar but not identical. We have planned acute studies in which we

will examine in detail the capacity of the array to excite neurons in different isofrequency lamina when the array is inserted into the nucleus from a more dorsal direction, so that the shanks will traverse the isofrequency lamina at a higher angle.

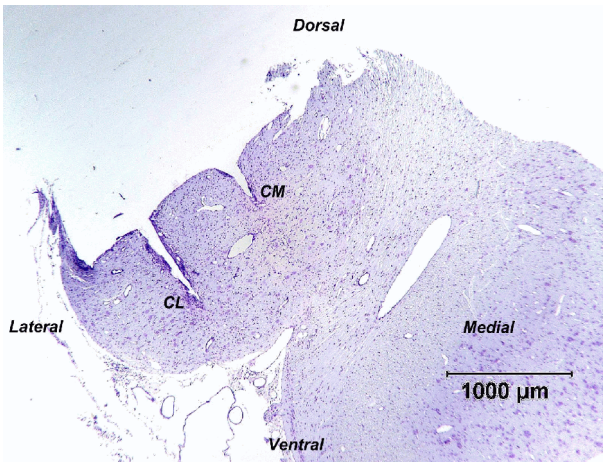

Fig 5-A

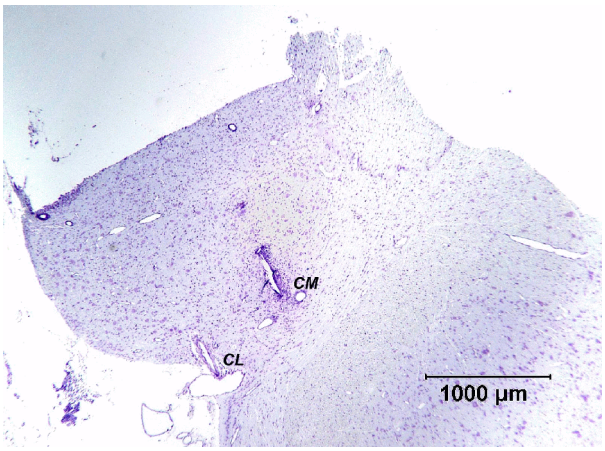

Fig 5-B

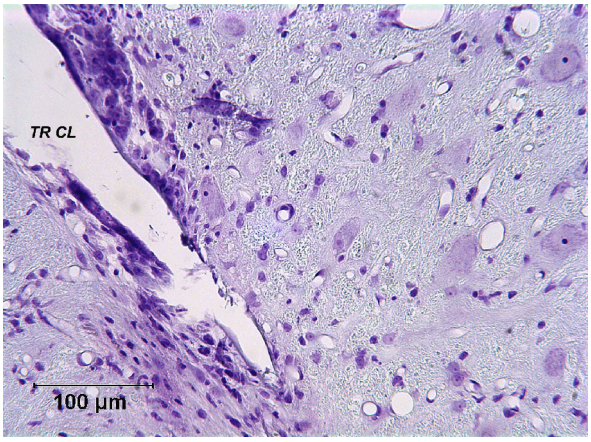

Fig 5-C

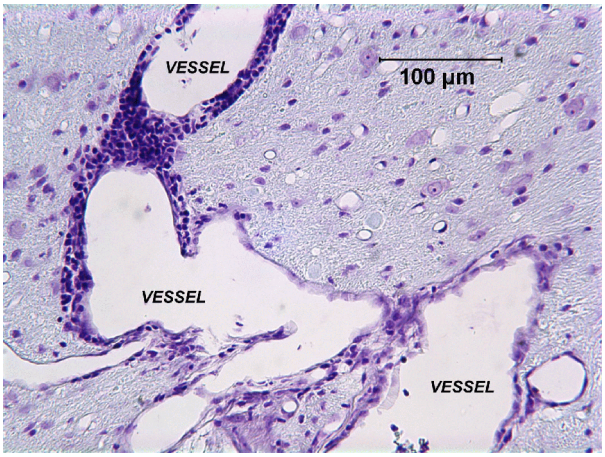

Fig 5-D

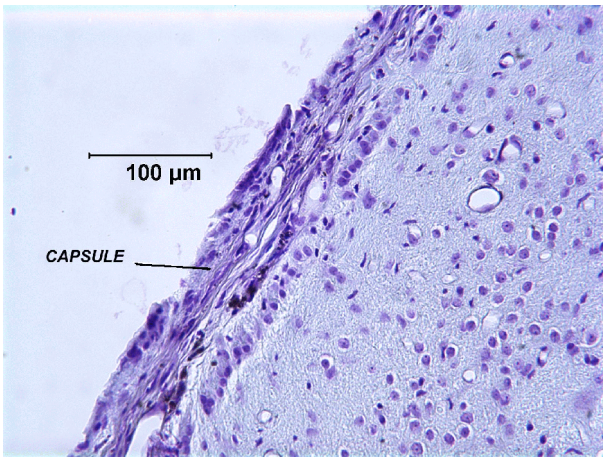

Fig 5-E

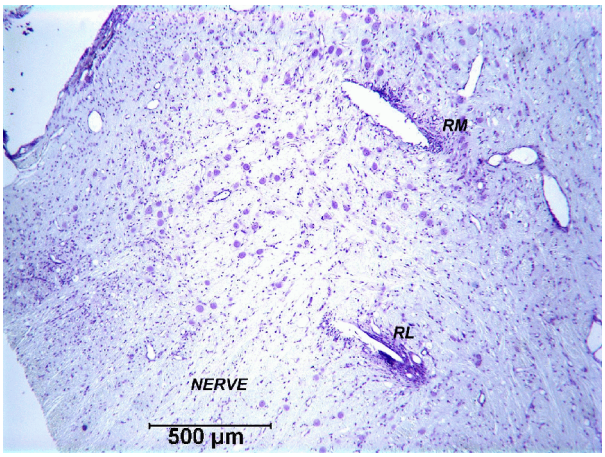

Fig 5-F

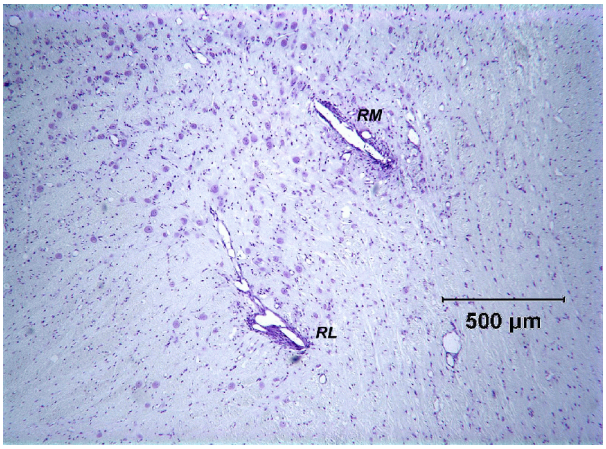

Fig 5-G

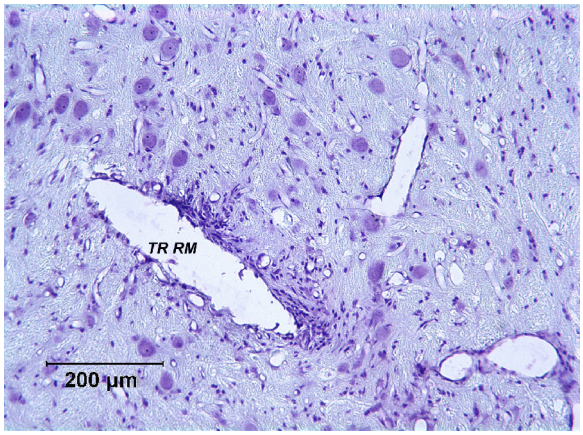

Fig 5-H

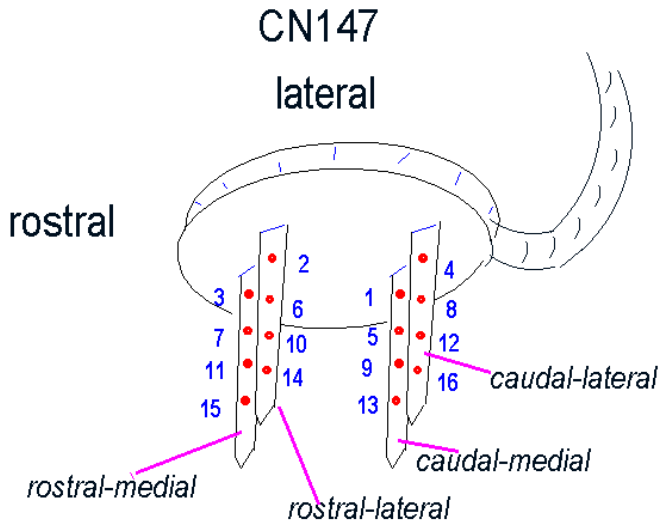
CN147
lateral
rostral
2
3
6
7
10
11
14
15
1
4
8
5
12
9
16
13
caudal-lateral
caudal-medial
rostral-medial
rostral-lateral

Fig 6

Caudal-lateral shank	caudal-medial shank
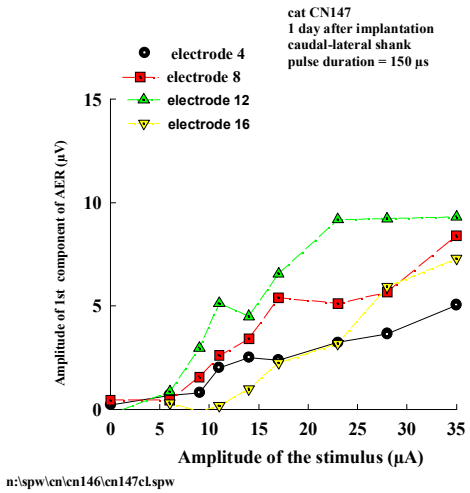 Fig 7-A	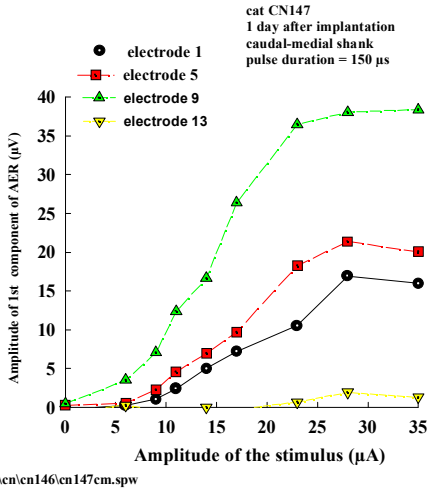 Fig7-C
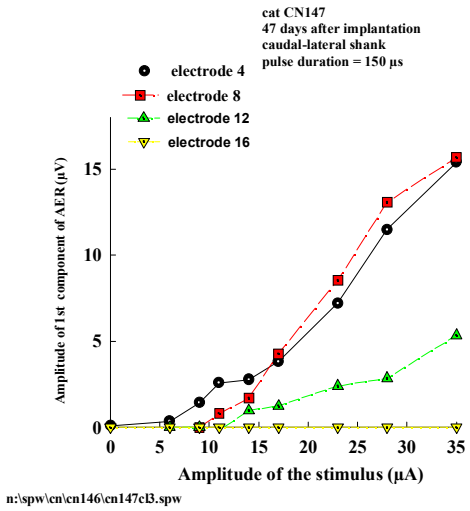 Fig 7-B	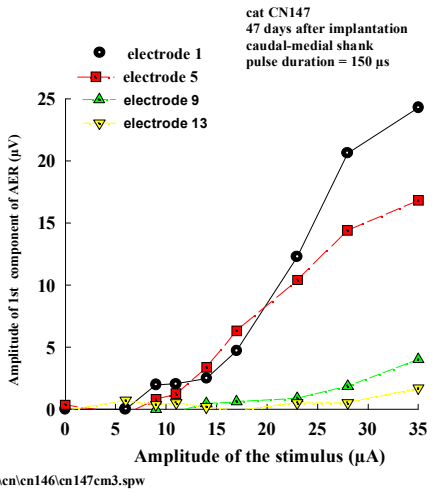 Fig 7-D

Rostral-lateral	Rostral-medial
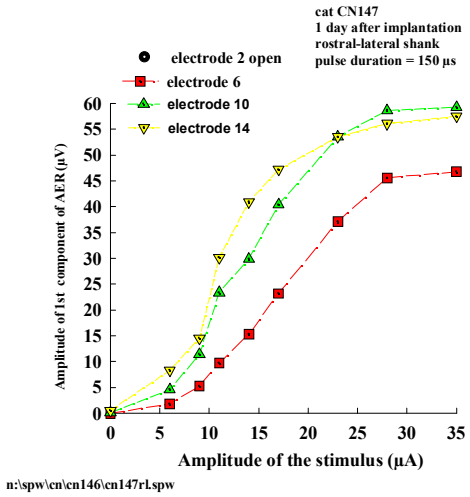	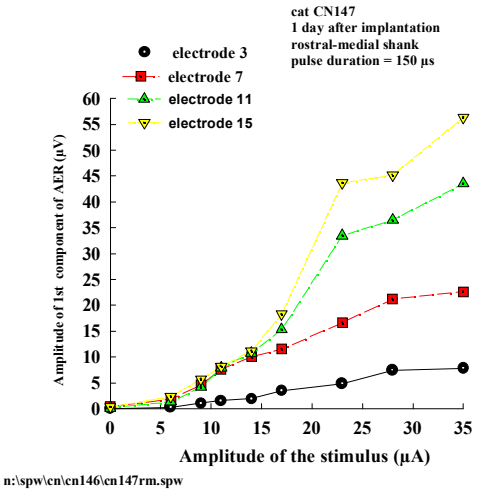
Fig 7-E	Fig 7-G
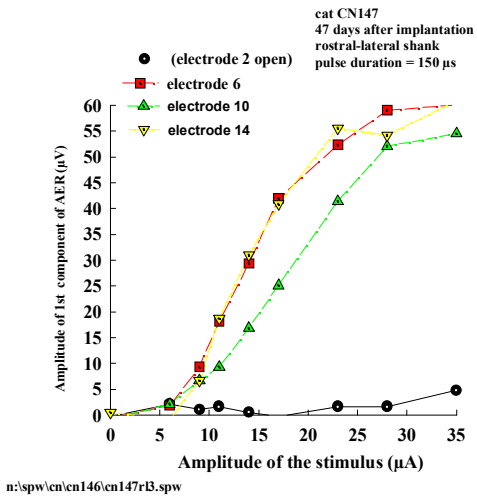	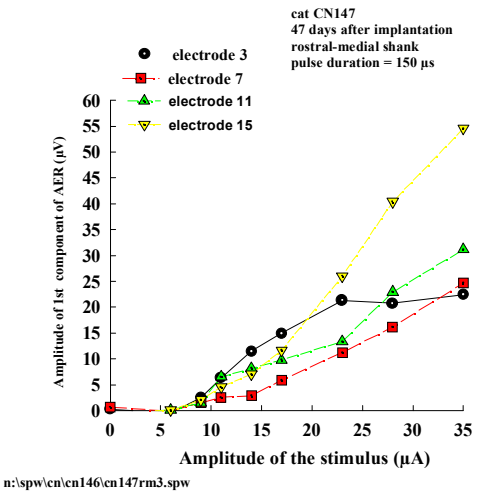
Fig 7-F	Fig 7-H

electrode site 8 (caudal-lateral)	electrode site 11 (rostral-medial)
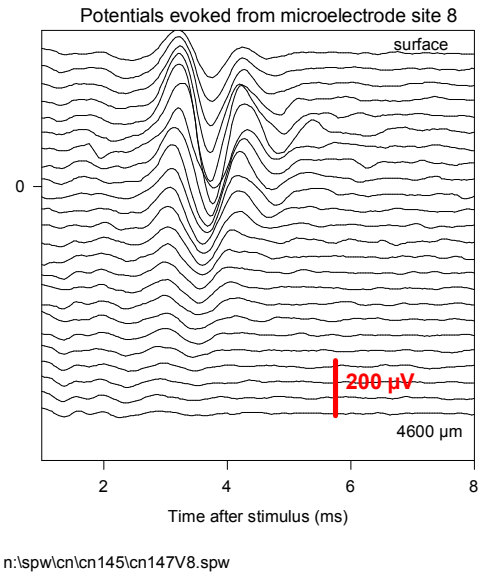 Fig 8-A	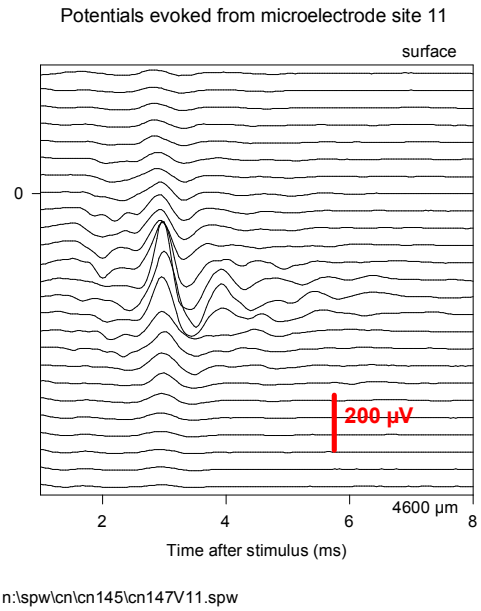 Fig 8-B

caudal -lateral	caudal-medial
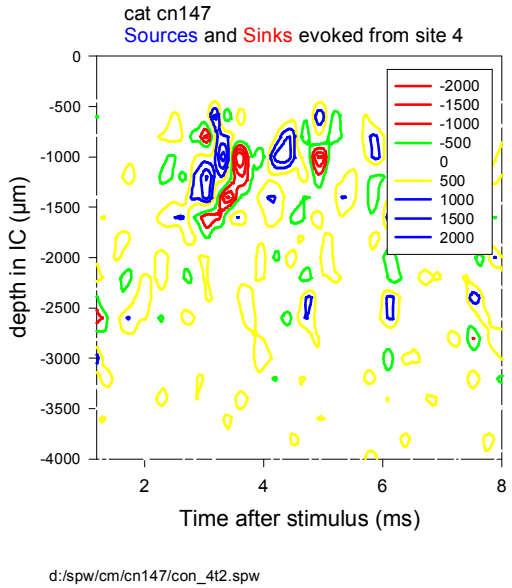	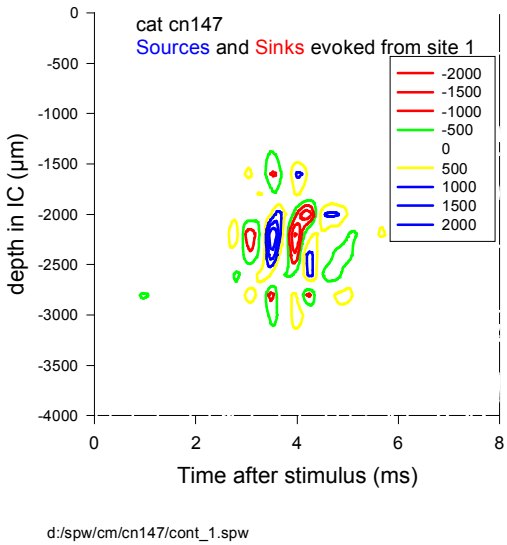
Fig 9-A	Fig 9-C
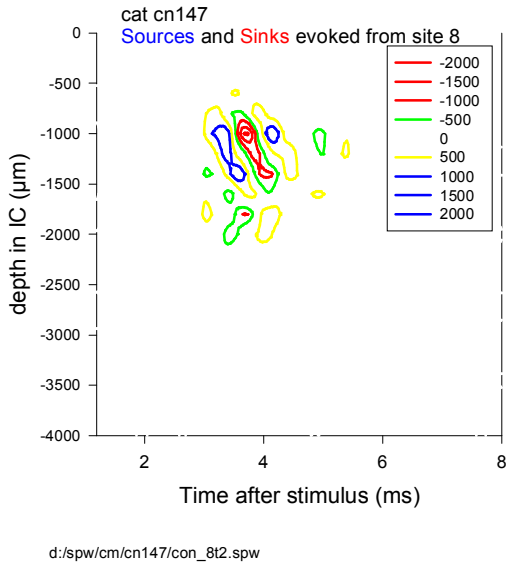	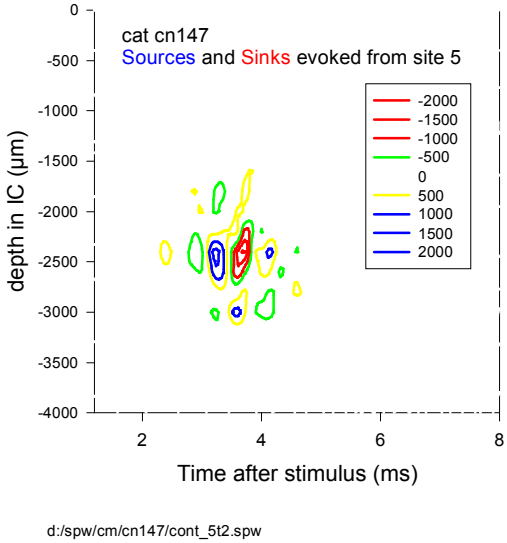
Fig 9-B	Fig 9-D

rostral-lateral	rostral-lateral (continued)
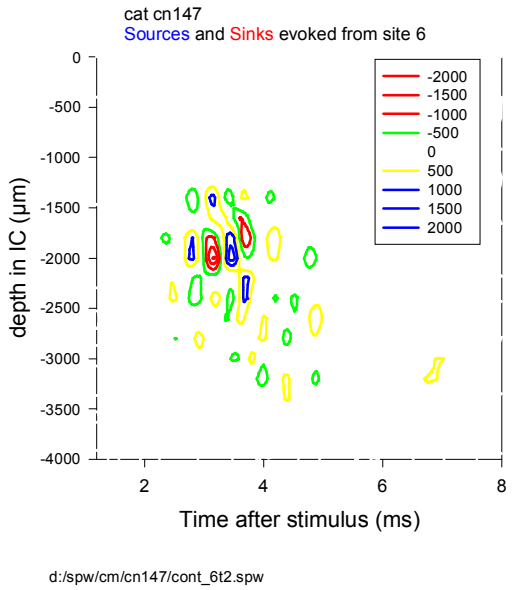 Fig 9-E	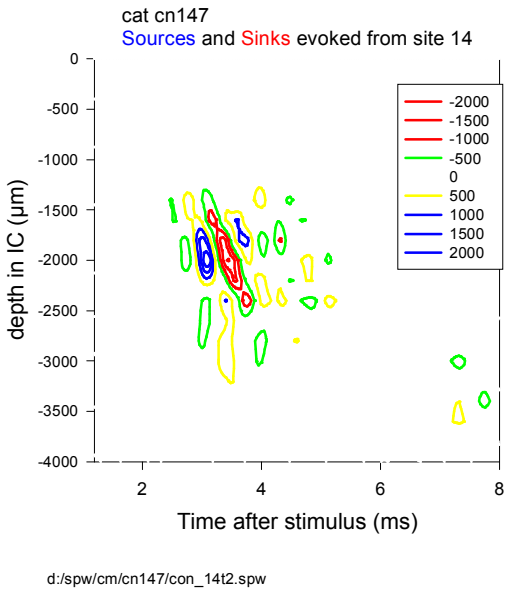 Fig 9-G
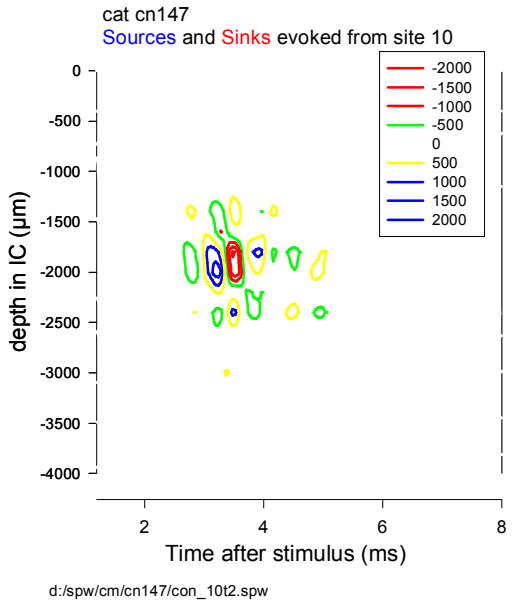 Fig 9-F	

rostral-medial	rostral-medial (continued)
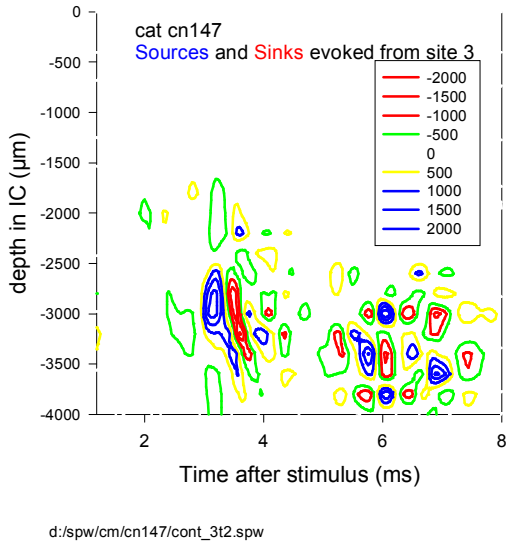	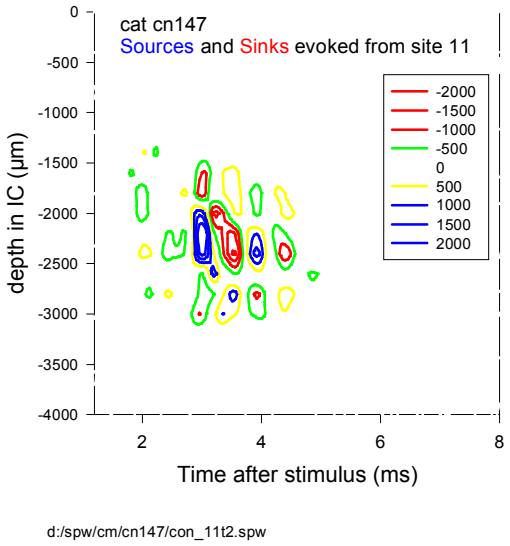
Fig 9-H	Fig 9-J
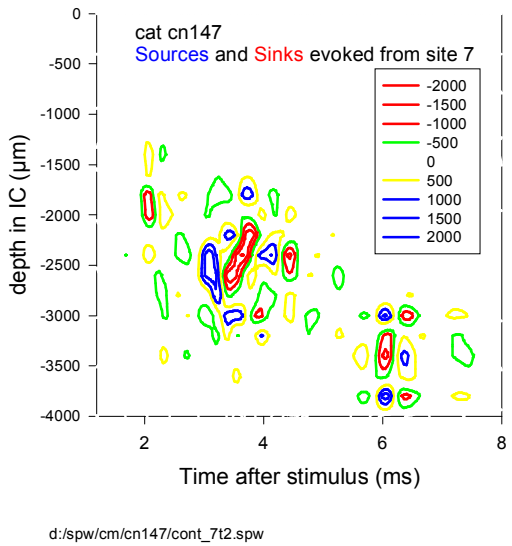	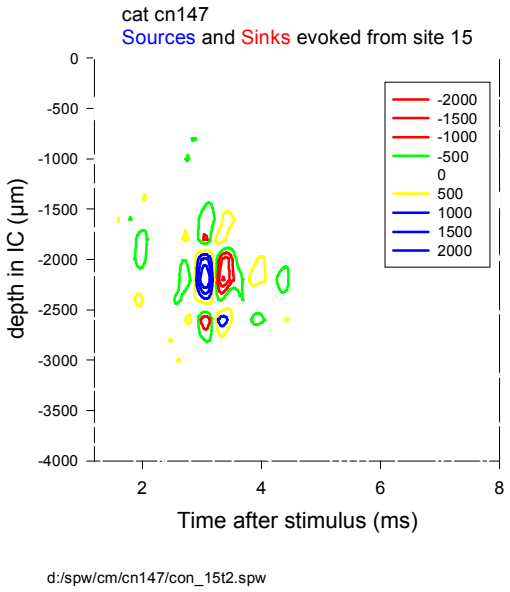
Fig 9-I	Fig 9-K

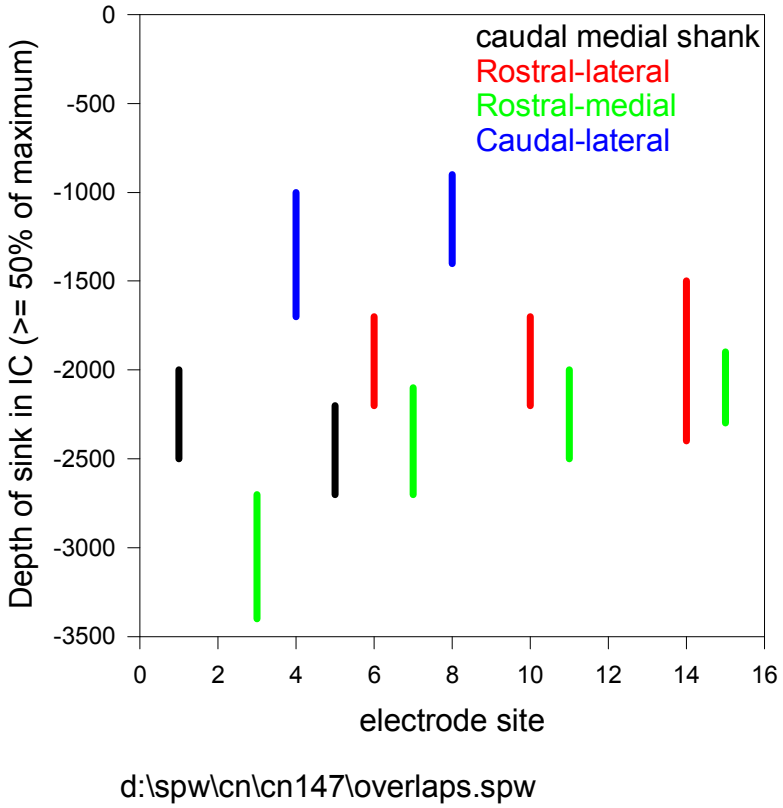
caudal medial shank
Rostral-lateral
Rostral-medial
Caudal-lateral
Depth of sink in IC (>= 50% of maximum)
0
-500
-1000
-1500
-2000
-2500
-3000
-3500
0
2
4
6
8
10
12
14
16
electrode site
d:\spw\cn\cn147\overlaps.spw

Fig 10

REFERENCES CITED

M. Brown, W.R Webster and R.L, Martin, “ The three-dimensional frequency organization of the inferior colliculus of the cat: a 2-deoxyglucose study”. *Hearing Research vol. 104 pp 57-73,* 1997.

J. A. Freeman and C. Nicholson, "Experimental optimization of current source-density technique for anuran cerebellum," *J Neurophysiol*, vol. 38, pp. 369-82., 1975

D. M. Harris, "Current source density analysis of frequency coding in the inferior colliculus," *Hear Res*, vol. 25, pp. 257-66, 1987.

P.A. Leake and R.L Snyder. “Topographic organization of the central projections of the spiral ganglion in cats,” *J Comp Neurol*, vol. 281, pp. 612-629, 1989

D. B. McCreery, R. V. Shannon, J. K. Moore, and M. Chategee, "Accessing the tonotopic organization of the ventral cochlear nucleus by intranuclear microstimulation," *IEEE Transactions on Rehabilitation Engineering*, vol. 23, pp. 391-399, 1998.

M.N. Semple and L.M. Aitkins. “ Representation of sound frequencies and laterality by units in the central nucleus of cat inferior colliculus”, *J. Neurophysiology, vol. 42 pp. 1629-1639, 1979*

R. L. Snyder and P. A. Leake, "Topography of spiral ganglion projections to cochlear nucleus during postnatal development in cats," *J Comp Neurol*, vol. 384, pp. 293-311, 1997.

R. L. Snyder, P. A. Leake, and G. T. Hradek, "Quantitative analysis of spiral ganglion projections to the cat cochlear nucleus," *J Comp Neurol*, vol. 379, pp. 133-49, 1997.